Rheo-NMR studies of the behavior of a nematic liquid crystal in a low-shear-rate regime: The transition from director alignment to reorientation

C. Lepper,[1] P. J. B. Edwards,[1] E. Schuster,[1] J. R. Brown,[2] R. Dykstra,[3] P. T. Callaghan,[3,4] and M. A. K. Williams[1,4]
[1]*Institute of Fundamental Sciences, Massey University, Palmerston North, New Zealand*
[2]*Department of Chemical and Biological Engineering, Montana State University, Bozeman, Montana 59717-3920, USA*
[3]*School of Chemical and Physical Sciences, Victoria University of Wellington, Wellington, New Zealand*
[4]*MacDiarmid Institute for Nanotechnology and Advanced Materials, Wellington, New Zealand*
(Received 12 June 2010; published 29 October 2010)

Deuterium NMR spectroscopy has been used to study the director dynamics of the nematic liquid-crystal system cetyl trimethylammonium bromide/D_2O under the action of applied viscous torques. Shear forces were applied using a custom-built Couette cell that was introduced into an NMR superconducting magnet, so that its rotational axis was parallel to the magnetic field direction, along which the liquid-crystal director originally aligned. Subsequently, the inner cylinder of the cell was rotated continuously at different rates using a stepper motor. The resulting time evolution and ultimate steady-state orientation of the director, governed by the competition between the applied viscous torque with elastic and magnetic terms, was measured via observed changes in the deuterium spectrum. Using a simple gearbox allowed unprecedented access to a low-shear-rate regime in which, above a threshold shear rate, the director of part of the sample was observed to reorient, while the remaining part still aligned with the magnetic field. Subsequent increases in the applied rotational rate were found to increase the relative proportion of the orienting fraction. Spatially resolved NMR spectra showed that the orienting and field-aligned fractions formed separated bands across the gap of the Couette cell, with director reorientation being initiated at the moving inner wall. The behavior was found to be consistent with the often ignored variation in velocity gradient manifest across the gap of a cylindrical cell, so that as the angular frequency of the inner cylinder was increased the radial location of the critical shear rate required for reorientation traversed the gap. Once the applied rotational rate was sufficient to reorient the director of the entire sample, the dependence of the exhibited steady-state orientation on the average applied shear rate was measured. These results could be fitted to an analytical solution of the force-balance equation, made tractable by the assumption that the elasticity term was of minor significance and could be ignored. Additionally, the use of a numerical solution of the full force-balance equation, which explicitly includes elasticity and secondary flow and additionally allows the time evolution of the director orientation to be calculated, was investigated.

DOI: 10.1103/PhysRevE.82.041712 PACS number(s): 83.80.Xz, 47.57.Lj, 47.57.Qk, 82.70.Uv

I. INTRODUCTION

The rheological behavior of nematic liquid crystals can exhibit a plethora of interesting phenomena, epitomized perhaps by the nematodynamics that occurs under the influence of external fields [1,2]. Not only are these systems of great interest in their own right, in particular owing to the nonlinear response of the material to applied shear stresses, but—in addition—such systems have both biomimetic and technological relevance [3,4]. Understanding how to manipulate the director orientation permits, for example, the optical properties of the material to be controlled by the experimenter, an ability that clearly harbors potential for use in an array of smart material and sensor applications.

A theory that describes the macroscopic response of a uniaxial liquid-crystal to a velocity gradient was first proposed by Ericksen during the 1960s [5]. This theory was subsequently applied to nematic fluids by Leslie [6] and describes how the imposition of a simple shear flow on a nematic phase can exert a viscous torque on the director. Such viscous torques are opposed by the elasticity of the phase, with the competition between the two terms yielding either alignment, where the director aligns with the streamline, or tumbling where the director continually rotates. In both flow-aligning and tumbling regimes the addition of further torques induced by external force fields can lead to instability of the flow, resulting in more complex director movement. Nematodynamic equations describe the resulting director dynamics in a number of different system configurations of this type [7–15]. Where a steady-state director orientation arises and the elastic torques are of minor significance, its shear-rate dependence can be described by a simple analytical expression, and the problem simplifies to that of an aligning external field in competition with shear [16]. However, attempting a more general solution of the coupled system of equations that describe the interaction of all three terms, where the elasticity of the nematic phase that resists deformation is included, reveals that in order to account for the emergence of a macroscopic steady-state director orientation, as observed in experiment, the introduction of a secondary flow is required [17].

Herein, deuterium NMR spectroscopy has been used to study the director dynamics of the nematic liquid-crystal system cetyl trimethylammonium bromide (CTAB)/D_2O under the action of an aligning magnetic field and applied viscous torques. The resulting time evolution and ultimate steady-state orientation of the director were measured via changes observed in the deuterium spectrum. The study focuses on a hitherto largely ignored low-shear-rate regime in which the possible presence of a threshold shear rate, only above which

does shear-induced reorientation occur, has been investigated. In addition, where orientation of the director is found the results have been modeled both analytically, by assuming that the elastic term is negligible, and with a numerical solution to the full coupled equations, and the outcomes are compared.

II. THEORY

When a stress is applied to a nematic liquid-crystal system the resultant strain rate behavior is related to the stress tensor through the six so-called Leslie viscosity coefficients $(\alpha_1-\alpha_6)$ [1,6]. The geometry of the system determines which of the six coefficients contribute to the effective viscosity in the direction of shear. When shear is applied by the rotation of the inner cylinder of a cylindrical Couette cell to a nematic phase whose director is coaxial with the Couette cell, viscous torques can only be generated when thermal fluctuations tip the director away from colinearity with the cell axis. Such random fluctuations subject the director to a torque of the same sign as α_2, and subsequently the applied force generates a new torque on the reoriented director of the same sign as α_3. For systems with $\alpha_3/\alpha_2<0$ this torque amplifies the initial fluctuation, destabilizing the director orientation and generating a homogenous deformation of the director field where all the micelles in the cell rotate in the same direction: the flow-alignment regime.

However, in the presence of a magnetic field the director dynamics are governed by the balance of three major terms: the viscous, elastic, and magnetic torques. When the shear rate is decreased below a critical shear rate, the hydrodynamic fluctuations are not expected to overcome elastic and magnetic torques, and as a result no instabilities are observed and the director remains aligned. Above this shear rate, however, a new steady-state director orientation is expected to result. In this regime, if the elasticity of the liquid-crystal phase is of minor significance and can be ignored, the shear-rate dependence of the steady-state angle Θ is given simply by

$$\tan(\Theta) = -\frac{\chi_a H^2}{2\mu_0|\alpha_3|\dot{\gamma}} + \sqrt{\left(\frac{\chi_a H^2}{2\mu_0\alpha_3\dot{\gamma}}\right)^2 + \left|\frac{\alpha_2}{\alpha_3}\right|}, \quad (1)$$

with χ_a being the diamagnetic anisotropy, H the magnetic field strength, μ_0 the vacuum permeability, $\dot{\gamma}$ the average shear rate, and $\alpha_{2,3}$ the Leslie coefficients. In the most general case, where all terms are kept, a set of equations that describe the time evolution of the director steady-state orientation for the relevant experimental geometry are given in [17]. A brief outline of this hydrodynamic model is as follows.

A point inside the cell is defined by a cylindrical coordinate system (r,θ,z), with $R_i \le r \le R_o$, $0 \le \theta \le 2\pi$, and $0 \le z \le d$, where R_i and R_o are the inner and outer radii of the respective cylinders of the Couette cell and $d=R_o-R_i$. The director is defined by $\mathbf{n}(r,\theta,z,t)=(n_r(r,\theta,z,t), n_\theta(r,\theta,z,t), n_z(r,\theta,z,t))$. Assuming that the velocity field can be obtained analytically by solving the Navier-Stokes equation for cylindrical Couette flow and neglecting inertial terms, the director equation is obtained from the torque balance equation:

$$\mathbf{k^e} + \mathbf{k^m} + \mathbf{k^v} = 0, \quad (2)$$

where $\mathbf{k^e}$, the elastic torque, is given by

$$\mathbf{k^e} = K\mathbf{n} \times \nabla^2\mathbf{n}, \quad (3)$$

$\mathbf{k^m}$ is the magnetic torque:

$$\mathbf{k^m} = \chi_a(\mathbf{n} \times \mathbf{H})(\mathbf{n} \cdot \mathbf{H}), \quad (4)$$

where χ_a is the diamagnetic anisotropy and $\mathbf{H} \equiv (0,0,H)$ is the magnetic field, and $\mathbf{k^v}$ is the viscous torque:

$$\mathbf{k^v} = -\mathbf{n} \times [\gamma_1(\dot{\mathbf{n}} - \Omega\mathbf{n}) + \gamma_2 A\mathbf{n}]. \quad (5)$$

The superposed dot denotes the material time derivative $\dot{\mathbf{n}} = \partial\mathbf{n}/\partial t + \mathbf{v}\cdot\nabla\mathbf{n}$; the following tensors, respectively, are the vorticity and rate-of-strain tensors:

$$\Omega := \tfrac{1}{2}[\nabla\mathbf{v} - (\nabla\mathbf{v})^T], \quad (6)$$

$$A := \tfrac{1}{2}[\nabla\mathbf{v} + (\nabla\mathbf{v})^T], \quad (7)$$

and γ_1 and γ_2 can be represented as linear combinations of Leslie viscosities $\gamma_1=\alpha_3-\alpha_2$ and $\gamma_2=\alpha_2+\alpha_3$.

The basic model has been developed further in order to include the effects of secondary flow, and indeed this was found in previous work to be necessary in order for the coupled equations described above to produce steady-state solutions for the director orientation [17]. Such secondary flows, subject to appropriate constraints, can be introduced by setting radial and longitudinal components of the velocity, $v_r=[-F(r)/r][dI(z)/dz]$ and $v_z=(1/r)[dF(r)/dr]I(z)$, respectively, where $F(r)$ is a function of r subject to the restrictions $F(R_i)=F(R_o)=0$ and $[dF(r)/dr]_{r=R_i}=[dF(r)/dr]_{r=R_o}=0$ and $I(z)$ is an arbitrary function of z [17].

Finally, after introducing the two polar angles Θ and Φ, such that the director components read $n_r=\sin\Theta\cos\Phi$, $n_\theta=\sin\Theta\sin\Phi$, and $n_z=\cos\Theta$ and after some algebraic manipulation, the general equations of motion for the director can be written in the following way:

$$\begin{aligned}\gamma_1\frac{\partial\Phi}{\partial t} = \frac{1}{2r^2}\Bigg\{ & 2\gamma_2\Bigg[AB\cos 2\Phi + \sin 2\Phi \\ & \times\left(2F(r) - r\frac{dF(r)}{dr}\right)\frac{dI(z)}{dz}\Bigg] + \sin\Phi\cot\Theta \\ & \times\Bigg[(\gamma_1+\gamma_2)I(z)\left(-\frac{dF(r)}{dr} + r\frac{d^2F(r)}{dr^2}\right) \\ & + (\gamma_1-\gamma_2)rF(r)\frac{d^2I(z)}{d^2z}\Bigg] \\ & - 2\gamma_1\Bigg[AB + rI(z)\frac{dF(r)}{dr}\frac{\partial\Phi}{\partial z} + B(A-Cr^2)\frac{\partial\Phi}{\partial\theta} \\ & - rF(r)\frac{dI(z)}{dz}\frac{\partial\Phi}{\partial r}\Bigg]\Bigg\} + K^e_\Phi, \end{aligned} \quad (8)$$

$$\gamma_1 \frac{\partial \Theta}{\partial t} = -\frac{1}{4r^2}\Bigg\{-\gamma_2 \sin 2\Theta\Bigg[2AB \sin 2\Phi + \left(r(3+\cos 2\Phi)\frac{dF(r)}{dr} - 2\cos 2\Phi F(r)\right)\frac{dI(z)}{dz}\Bigg] - 2\gamma_2 r \cos\Phi \cos 2\Theta F(r)\frac{d^2I(z)}{dz^2} + 2I(z) \times\Bigg[\cos\Phi(\gamma_1+\gamma_2\cos 2\Theta)\left(-\frac{dF(r)}{dr}+r\frac{d^2F(r)}{dr^2}\right) + 2\gamma_1 r\frac{dF(r)}{dr}\frac{\partial\Theta}{\partial z}\Bigg] + 2\gamma_1\Bigg[2B(A-Cr^2)\frac{\partial\Theta}{\partial\theta} + rF(r) \times\left(\cos\Phi\frac{d^2I(z)}{dz^2} - 2\frac{dI(z)}{dz}\frac{\partial\Theta}{\partial r}\right)\Bigg]\Bigg\} - \frac{\chi_a H^2}{2}\sin 2\Theta + K_\Theta^e, \tag{9}$$

where the terms for the elastic torques read

$$K_\Phi^e = K\{\sin\Phi[\sin\Theta \sin\Phi(\nabla^2\mathbf{n})_z - \cos\Theta(\nabla^2\mathbf{n})_\theta] - \cos\Phi[\cos\Theta(\nabla^2\mathbf{n})_r - \sin\Theta\cos\Phi(\nabla^2\mathbf{n})_z]\}, \tag{10}$$

$$K_\Theta^e = K\sin\Theta[\cos\Phi(\nabla^2\mathbf{n})_\theta - \sin\Phi(\nabla^2\mathbf{n})_r], \tag{11}$$

and $(\nabla^2\mathbf{n})_i$ denotes the Laplacian of the director components in cylindrical coordinates. Equations (8) and (9) provide a full three-dimensional hydrodynamic model of the experimental situation described herein, with periodic boundary conditions in the z direction, and allow the time evolution of the director to be calculated with the possibility of including elasticity and secondary flow. These equations were solved numerically using a finite-element solver. Solutions were computed on the cylindrical domain with 5000 degrees of freedom using the application of a variable-order, variable-step-size, and backward differentiation formalism. On both the inner and the outer cylinder surfaces Dirichlet boundary conditions were applied, keeping the director orientation aligned with the magnetic field at all times to mimic wall anchoring.

III. EXPERIMENTAL DETAILS

The chosen CTAB/D_2O system was studied with the use of a rheo-NMR apparatus that combines the ability to obtain information about the molecular orientation of the liquid-crystalline system afforded by NMR spectroscopy of the quadrupolar ^{2}H nucleus with the ability to carefully control applied shear rates. This has made it possible to study the behavior of the system under shear in the presence of a strong static magnetic field [18].

CTAB is an amphiphilic molecule comprised of a hydrophilic polar head group and a hydrophobic hydrocarbon tail. These molecules self-assemble in water to form wormlike micelles (WLMs) which self-organize into temperature- and concentration-dependent liquid-crystal phases which are characterized by their level of orientational and translational

FIG. 1. (Color online) The self-assembly of CTAB molecules into a micelle, the self-organization of those micelles into a liquid-crystal nematic phase, and subsequent alignment by a magnetic field.

orders. A 20 wt % CTAB solution at a temperature of 305 K forms a nematic phase of WLMs [18] (Fig. 1). When placed in a magnetic field the individual domains align with their directors parallel to the direction of the field.

Rheo-NMR has proven to be a valuable technique in the study of liquid-crystal systems [19]. In the CTAB system studied herein D_2O is used as a solvent and additionally acts as an NMR probe, allowing ^{2}H-NMR techniques to be used to monitor the response of the sample during the experiments. When all the WLMs are aligned, the ^{2}H-NMR spectrum is a single Lorentzian doublet of the form

$$\text{Intensity} \propto R_2/[(\nu \pm 0.5\nu_Q)^2 + (R_2)^2], \tag{12}$$

with R_2 being the linewidth at half-height and $\nu_Q = (3/4)e^2qQ/h[3\cos^2\Theta(t)-1]$, so that the peak-to-peak splitting of the doublet is dependent on the director orientation $\Theta(t)$ of the liquid crystal with respect to the magnetic field:

$$\delta\nu(t) = \delta\nu_0[3\cos^2\Theta(t) - 1]/2, \tag{13}$$

where $\delta\nu_0$ is the line splitting of the spectrum when the WLMs are aligned with the magnetic field [where $\Theta(0) = 0°$]. When multiple alignments are present in one sample, the resultant spectra are an appropriately weighted sum of doublets.

The rheo-NMR experiments were performed on samples in a custom-built Couette cell which fitted into a 500 MHz NMR probe head [20] (Fig. 2). The Couette cell was constructed from two glass NMR tubes which were used to create two concentric cylinders with axes parallel to the magnetic field of the NMR magnet. A 3 mm outside diameter NMR tube placed inside a 5 mm outside diameter thin-walled NMR tube and was supported by two PEEK fittings which held the tubes coaxial. The outer tube was fixed in place, while the inner tube was linked via a nonmagnetic shaft to an external stepper motor mounted on top of the magnet. The annulus was filled to a depth of 50 mm with the CTAB sample and positioned in the detection zone of the NMR coil (Fig. 2). The rheo-NMR experiments where performed over a wide range of shear rates at 305 K. The temperature was controlled ±1 K by a conventional gas-flow system. Herein we report the results obtained by varying the rotation rate of the inner cylinder between ~0.0004 and 0.1 Hz, corresponding to gap-averaged shear rates ranging from 0.0072 to 1.80 s^{-1}. Samples were left to equilibrate for 45 min after insertion into the field before shear was applied. Subsequently, deuterium spectra were then recorded until they appeared to have reached a steady state (typically 30

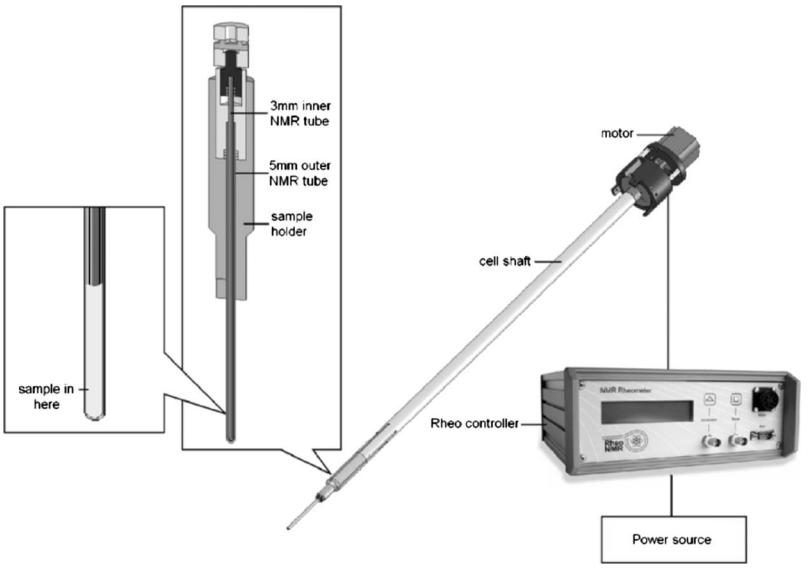

FIG. 2. Schematic of the NMR Couette shear cell used in this work, illustrating (from left to right) the sample tube, its incorporation into a spinner-type housing with the inner tube attached to an external coupling, and finally the attachment of this housing to the cell shaft, which could be introduced in the magnet bore and driven to rotate via the stepper motor.

min). The signal-to-noise ratio was sufficiently large such that only one scan had to be performed to obtain each of the spectra.

In order to obtain deuterium spectra as a function of position within the Couette fluid gap, one-dimensional (1D) magnetic-resonance imaging was performed [21] on a Bruker AVANCE 400 spectrometer with a 9.4 T superconducting 89 mm vertical bore magnet and a Micro 2.5 imaging probe. To obtain sufficient signal-to-noise ratio for spatial resolution, a larger volume rheo-NMR Couette device was constructed as described above, but with a 15 mm outer diameter glass NMR tube fitted inside a 20 mm outer diameter tube, resulting in a fluid gap of 1.5 mm. In a simple spin-echo experiment of approximately 10 min duration, two soft rf pulses were used to selectively excite a 4×10 mm^2 region in the x-z plane. A phase encoding gradient was applied in the y direction to encode spatially with a pixel resolution of ~ 200 μm while still maintaining spectral resolution. 1D spatially resolved deuterium spectra were collected for a gap-averaged shear rate of 0.02 s^{-1} at a temperature of 305 K.

IV. RESULTS AND DISCUSSION

Figure 3 shows the ^{2}H spectrum obtained after the alignment of the CTAB nematic phase in the 11.7 T (500 MHz for ^{1}H NMR) magnetic field. The line shape is well described by a pair of Lorentzian lines as shown by the fit to Eq. (12) ($R^2=0.999$), which yields a peak-to-peak splitting of 21.615 ± 0.001 Hz and a linewidth at half-height of 1.299 ± 0.005 s^{-1}. The comparison of the value of the spin-spin relaxation time T_2 directly measured in the time domain following a series of quadrupolar echoes with that inferred from the linewidth as $(1/\pi T_2)$ suggests that around 10% of the linewidth results from a distribution in the director orientation. In turn, simulations of the effect of such a Gaussian distribution of the angle between the director and the magnetic field show that variances of greater than around 7° would produce a noticeable anisotropy in the line shape not visible in our experiments. Figure 4 shows the time evolution of the spectrum shown in Fig. 3 following the initiation of shear, with the rotation rate of the inner cylinder set at 0.0008 Hz. In this case it can be seen from the stability of the splitting that no detectable reorientation of the director is induced. This implies that, at this shear rate, the WLMs keep their unperturbed director orientation along the magnetic field and slip past one another in shear.

In contrast Fig. 5(a) shows that, on the application of an increased rotation rate of 0.0012 Hz, there is clear evidence of a dramatic change in the ^{2}H spectrum corresponding to shear-induced reorientation which appears to reach a steady state within approximately 15 min. It is interesting to note that only part of the sample exhibits this reorientation behavior (indicated by the appearance of a new doublet with narrower splitting), while a substantial amount of the sample still has a director oriented along the magnetic field direction and exhibits the initial zero-shear splitting of the ^{2}H doublet. On increasing the rotation rate further to 0.0016 Hz, and subsequently to 0.0018 Hz, the proportion of the sample still aligned along the static field direction can be observed to reduce [Figs. 5(b) and 5(c)]; until upon the application of

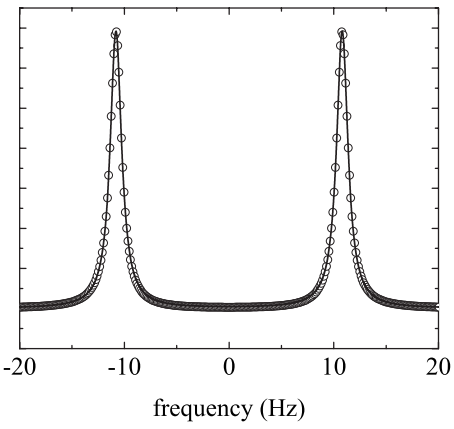

FIG. 3. Experimental deuterium NMR spectra of a 20% CTAB/D_2O recorded at 11.7 T and 305 K. The solid line is a fit as described in the text.

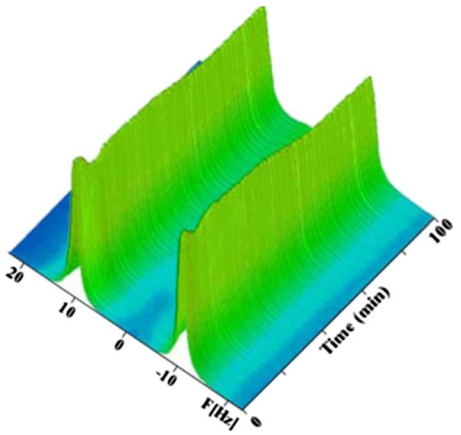

FIG. 4. (Color online) Deuterium NMR spectra of 20% CTAB/D_2O at 305 K, measured in the 500 MHz NMR superconducting magnet, when the inner cylinder is continually rotated at 0.0008 Hz, giving a gap-averaged shear rate of 0.014 s^{-1}.

rotation rate of 0.0020 Hz the entire sample now reorients. Figure 6 shows the resultant spectrum upon application of 0.04 Hz, and the recorded spectrum is now well described by a single pair of Lorentzian lines once more, as shown by the another fit to Eq. (12) (R^2=0.998), yielding a peak-to-peak splitting of 6.27 ± 0.01 Hz and a linewidth at half-height of 2.41 ± 0.01 s^{-1}.

In order to investigate further the competition between the applied viscous torques and that arising from the magnetic field, the experiment carried out at a rotational rate of 0.0008 Hz, where no orientation of the director was observed with time at 11.7 T [Figs. 4 and 7(a)], was repeated at 9.4 T using the superconducting magnet routinely used for 400 MHz NMR spectroscopy. It is clear that at this weaker field strength shearing at this rate *is* now capable of generating reorientation of the director [Fig. 7(b)].

Subsequently in order to understand the origin of the two splittings observed at intermediate shearing rates (between that at which shearing is insufficient to reorient the director at all and that at which the entire sample reorients), experiments were carried out directly probing the spatial distribution of alignment in the sample in this regime. Initially heterogeneities in the z direction owing to phenomena such as demixing were discounted by examining the spectra within selected slices along the z axis, which showed no change with respect to position. Then, spectrally resolved 1D imaging experiments were carried out in a 9.4 T spectrometer equipped with an imaging probe as described in the experimental section. After shearing for sufficient time to generate a steady-state spectrum (whose spectrum averaged across the gap was clearly two components), individual spectra were recorded spatially resolved across the gap, as depicted in Figs. 8(a) and 8(b). In order to limit experiment time and achieve the designed temporal resolution, spatial resolution was such that there were typically 6–7 pixels across the fluid gap. The results clearly show that the two orientational environments are spatially separated across the gap, with the director of the sample in the vicinity of the moving inner wall reoriented, while at the static outer wall the director is still aligned with the applied magnetic field.

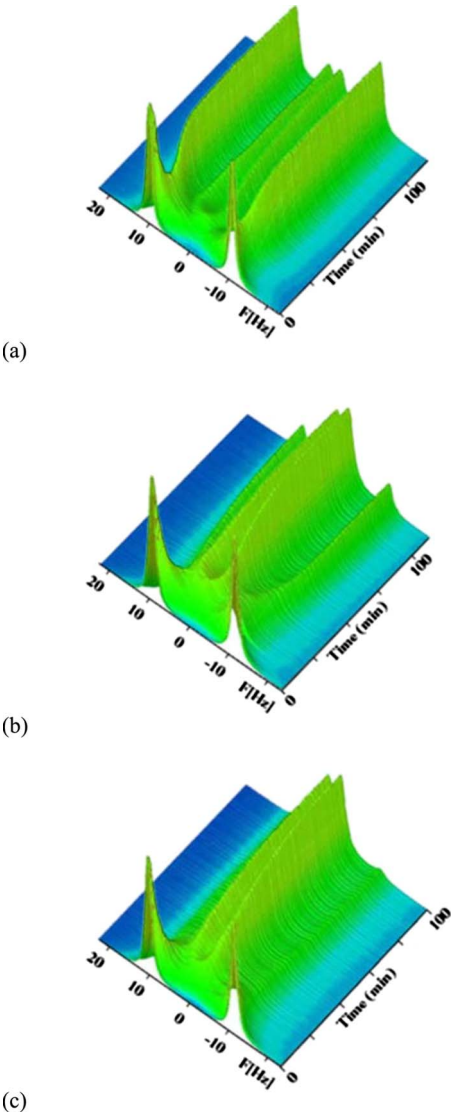

FIG. 5. (Color online) Deuterium NMR spectra of 20% CTAB/D_2O at 305 K with the inner cylinder rotating at (a) 0.0012 Hz (0.021 s^{-1}), (b) 0.0016 Hz (0.028 s^{-1}), and (c) 0.0018 Hz (0.031 s^{-1}) at 11.7 T (gap-averaged shear rates are given in brackets). Time equals zero indicates the initiation of shear. A growing proportion of the sample realigns along a new director as a result of the shear flow, while there rest of the sample remains aligned with the direction of the field.

It is suggested that the radial position at which the reorientation of the director is initiated in the Couette cell depends on where the locally applied shear rate exceeds some critical value. Indeed, even assuming a Newtonian flow curve different shear rates are applied across the gap in a cylindrical Couette geometry, as illustrated in Fig. 9 and by the following equations, which give the maximum and gap-averaged shear rates applied to the sample in this geometry as

$$\dot{\gamma}_{max} = \frac{2\omega}{1 - \left(\frac{R_i}{R_o}\right)^2}, \tag{14}$$

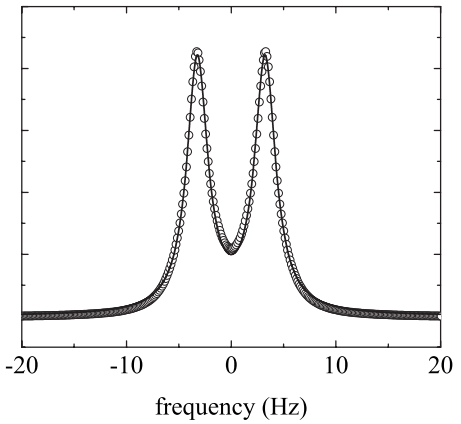

FIG. 6. Deuterium NMR spectra of a 20% CTAB/D_2O at 305 K, with the sample in the rheocell with the inner cylinder rotating at 0.04 Hz, giving a gap-averaged shear rate of 0.7 s^{-1}, measured at 11.7 T. The solid line is a fit described in the text.

$$\dot{\gamma}_{av} = \frac{4\omega\left(\frac{R_i}{R_o}\right)^2 \ln\left(\frac{R_i}{R_o}\right)}{\left[1-\left(\frac{R_i}{R_o}\right)^2\right]^2}, \tag{15}$$

respectively, where ω is the angular velocity of the rotating inner tube, and R_i and R_o are the inner and outer radii of the annulus [22].

The radial location of such a critical shear rate can then be calculated at a particular angular velocity of the inner cylinder simply by taking the relative intensity of the two ^2H doublets observed and relating this to the ratio of the volumes of inner and outer annuli (corresponding to flow- or field-aligned environments, respectively). Figure 9 shows plots of the calculated shear-rate profiles across the gap, formed in a number of experimental situations, and their intersections with the radii that correspond to the experimentally measured division between the different orientational environments (as inferred from the relative intensities of the two distinct ^2H doublets from a nonlinear least-squares fit). It can be seen that indeed for rotational rates of the inner cylinder above around 0.0012 s^{-1} this construction leads to the conclusion that within experimental uncertainties the assumption of a single critical shear rate 0.023 ± 0.002 s^{-1} is a reasonable description of the system. Here, the movement of the orienting band outward from the inner wall that occurs as the rotational rate of the inner cylinder is increased results from the movement of the radial position at which the critical shear rate is applied across the cell.

For the larger cell in which the spatially resolved spectra shown in Fig. 8 were obtained, the interface between the field-aligned and shear-orienting bands is found to occur at 8.13 ± 0.13 mm. From a calculation of the entire shear-rate profile across the gap, this radial position corresponds to a critical shear rate of 0.0206 ± 0.0007 s^{-1}, which can be seen to agree within experimental uncertainties with the value obtained from the smaller cell. Returning to Fig. 9, however, at the very lowest shear rates, corresponding to one rotation of the inner cylinder approximately taking over half an hour,

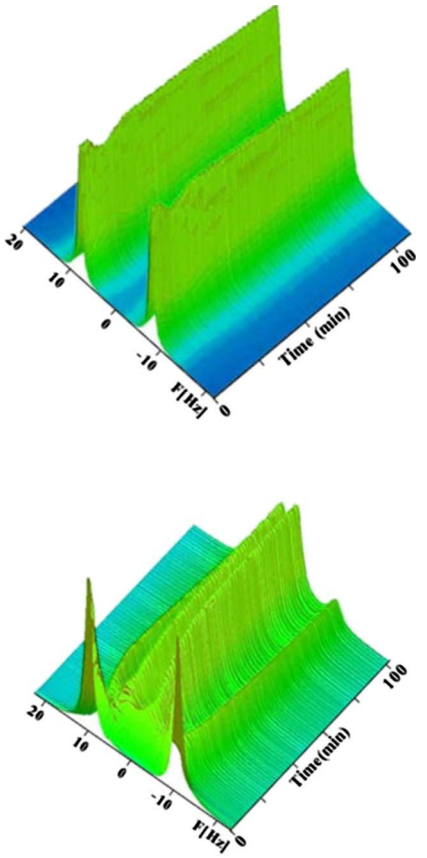

FIG. 7. (Color online) Deuterium NMR spectra of 20% CTAB/D_2O at 305 K with the inner cylinder rotating at 0.0008 Hz, giving a gap-averaged shear rate of 0.014 s^{-1}, in (a) the 500 MHz NMR superconducting magnet and (b) the 400 MHz NMR superconducting magnet. Time equals zero indicates the initiation of shear. While the larger magnetic field strength keeps the director aligned at this shear rate, the reduced field is less stabilizing which manifests a lower critical shear rate for reorientation.

there does appear to be some deviation from this behavior, which could possibly arise from complications associated with wall anchoring, slippage, or the non-Newtonian nature of the flow curve.

At applied rotational rates where the entire sample experiences shear rates above the critical value, reorientation of the whole sample occurs as shown in Fig. 6 and is well described by a single average director orientation. Increasing the shear rate in this regime was found to produce noticeable differences in the splitting of the single ^2H doublet, and data reflecting the change in the average angle of the director versus average shear rate could be extracted (Fig. 10). Also shown in Fig. 10 is a fit to Eq. (1) that can be seen to be a reasonable description of the system and provides two measured values for the Leslie viscosities of this WLM system. This indicates that in this regime the reorientation of the WLMs is well described by the theory used to describe the results of other nematic phases composed of polymers, which do not have the possibility of breakage and reformation afforded by the dynamic nature of the WLMs.

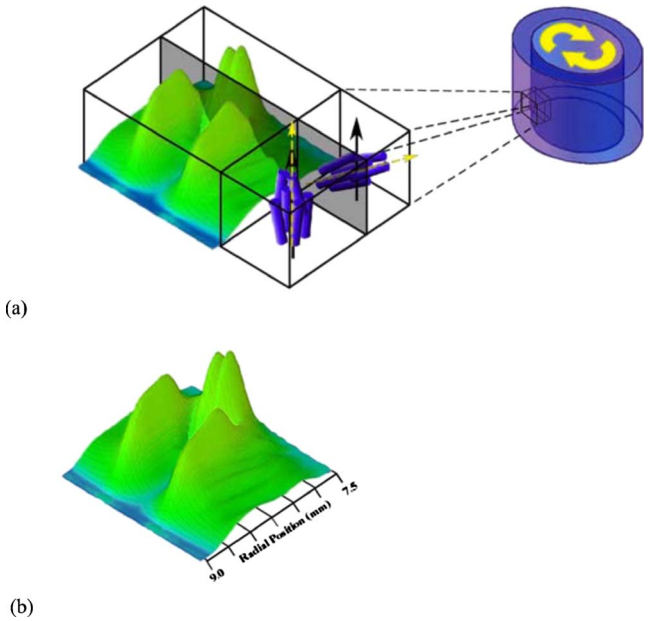

FIG. 8. (Color online) (a) and (b) Deuterium spectra measured at 305 K, spatially resolved across the cell gap after a dual-component steady state was achieved by continuously rotating the inner cylinder of the cell (for approximately 120 min) at an average shear rate of 0.02 s^{-1}. Results show that ~2/3 of the sample has remained aligned with the direction of the magnetic field, while approximately 1/3 of the sample near the inner wall of the cell has realigned along a director between the direction of the magnetic field and the direction of the shear flow.

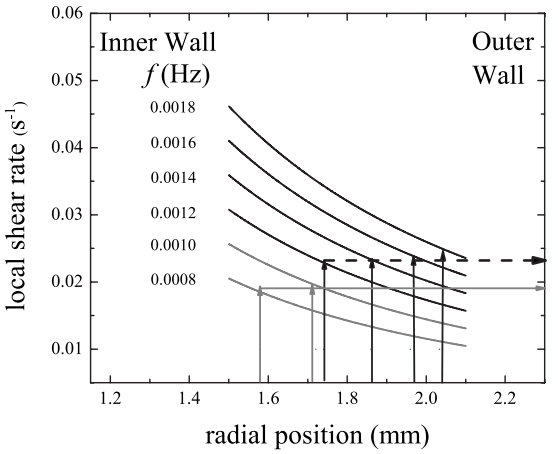

FIG. 9. Imposed shear-rate profiles across the gap of the cylindrical Couette cell as a function of the radii for different rotational rates (0.0008–0.0018 Hz) of the inner shaft. Arrows indicate the radial position within the cell that marks the boundary between the field and flow-aligned regions, as derived by the relative proportions of the two observed ^{2}H doublets exhibited at each rate. Within experimental uncertainties (typical uncertainty in radial position, ±0.0001 m, giving the corresponding local shear rate of ±0.002 s^{-1}) the four highest rates are consistent with a single critical shear rate.

Motivated by the possibility of obtaining more details, including the time evolution of the director orientation, a numerical simulation was also undertaken as described in Sec. II. This simulation includes the elasticity of the phase, neglected in the analytical approach, but consequently has been found to require a secondary flow to be included in order for the coupled equations to converge to steady-state solutions [17]. While it seems unclear that assuming the presence of such Taylor-type secondary flows is justified in the experimental case studied here, with the relevant Reynolds number <1, this general approach has the advantage of predicting the time dependence of the reorientation of the director after the initiation of shear [Eqs. (8) and (9)], which can be compared with experiment [Fig. 11(a)]. Subsequently, by repeating the simulation many times as a function of angular frequency, the dependence of the steady-state director orientation on average applied shear rate was also obtained from these computations [Fig. 11(b)]. As can be seen from Fig. 11 it was found that the experimentally determined functional forms of both the time and shear-rate dependences of the director orientation were described reasonably well by the numerical simulations. When using vanishingly small values of the elastic term and setting reasonably small radial and longitudinal velocities describing the secondary flow (~0.002 ms^{-1}), it was found that the Leslie coefficients required to give reasonable agreement of the simulation with the experimental measurements were within a factor of 2 of the values extracted by fitting the data to the analytical expression given by Eq. (1) as shown in Fig. 10. However, it should be noted that simulations carried out using larger secondary flows and/or higher values for the elasticity of the phase could also reproduce the experimental data reasonably by modifying the values of the Leslie coefficients used. If these parameters are not known independently, then any extraction of the Leslie coefficients by comparison of the experimental data to simulation should be performed with caution.

V. CONCLUSIONS

Deuterium NMR spectroscopy has been used to study the director dynamics of the nematic liquid-crystal system CTAB/D_2O under the action of applied viscous torques. The resulting time evolution and ultimate steady-state orientation of the director, governed by the competition of the applied viscous torque with elastic and magnetic terms, were measured via changes observed in the deuterium spectrum.

Using a simple gearbox allowed unprecedented access to a low-shear-rate regime and the measurement of a threshold shear rate above which the director of part of the sample was observed to reorient, while the remaining part still aligned with the magnetic field. Subsequent increases in the applied rotational rate were found to increase the relative proportion of the orienting fraction. Spatially resolved NMR spectra showed that these two fractions formed separated bands across the gap of the Couette cell, with director reorientation being initiated at the moving inner wall. This behavior was found to be consistent with the known variation in velocity gradient manifest across the gap of a cylindrical cell, so that as the angular frequency of the inner cylinder was increased

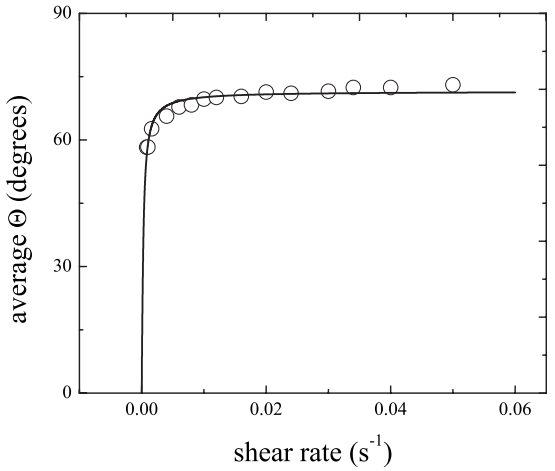

FIG. 10. Steady-state reorientation angle versus the average applied shear rate, together with a fit to Eq. (1), as described in the text, yielding Leslie coefficients $\alpha_2 = 1816 \pm 305$ Pa s and $\alpha_3 = 211 \pm 51$ Pa s.

the radial location of the critical shear rate required for reorientation traversed the gap.

At higher shear rates where the entire sample reoriented, data reflecting the change in average steady-state angle versus shear rate could be extracted. While a numerical solution of the full force-balance equation reproduced the time dependence of the director well for individual shear rates and additionally the dependence of the steady-state reorientation angle on shear rate, the Leslie coefficients required for this methodology to reproduce the experimental results were found extremely sensitive to both the magnitude of the elastic term and the presence and nature of secondary flow. If these parameters are not known independently, then any extraction of the Leslie coefficients made via comparison of the experimental data to simulation should be performed with caution. Alternatively, the steady-state director orientation versus shear-rate data could also be fitted, yielding reasonable values for two Leslie viscosities of this WLM system, to an analytical solution of the force-balance equations, made tractable by the assumption that the elasticity term was of minor importance and could be ignored. This indicates that in this regime the reorientation of the WLMs is well described by the theory used to describe the results of other nematic phases composed of polymers, which do not have the possibility of breakage and reformation.

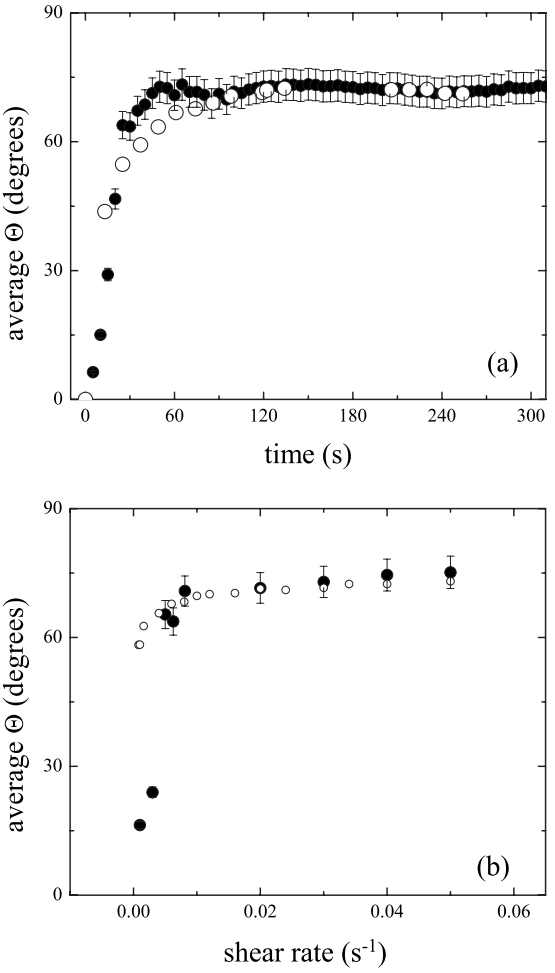

FIG. 11. (a) The experimentally measured time evolution of the director orientation after the initiation of the rotation of the inner cylinder at a rotational rate of 0.024 Hz, together with the results of a numerical simulation carried out as described in the text. (b) The resultant steady-state reorientation angle versus the average shear rate obtained from the numerical simulation, compared with experiment.

ACKNOWLEDGMENTS

The authors kindly acknowledge CSIRO Australia for providing support (E.S.), the U.S. National Science Foundation for funding (J.R.B.), and Magritek for financial support. Terry Southern and Steve Denby are thanked for their skillful assistance in the construction of the cell.

[1] M. Kleman and O. D. Lavrentovich, *Soft Matter Physics* (Springer-Verlag, Berlin, 2003).
[2] R. Ganapathy, S. Majumdar, and A. K. Sood, Phys. Rev. E **78**, 021504 (2008).
[3] A. J. McKinnon, Curr. Appl. Phys. **6**, 375 (2006).
[4] P. Oswald and P. Pieranski, *Nematic and Cholesteric Liquid Crystals* (Taylor & Francis, London, 2005).
[5] J. L. Ericksen, Arch. Ration. Mech. Anal. **4**, 231 (1960); **9**, 371 (1962).
[6] F. L. Leslie, Arch. Ration. Mech. Anal. **28**, 265 (1979); Adv. Liq. Cryst. **4**, 1 (1968).
[7] S. Chandrasekhar, *Liquid Crystals*, 2nd ed. (Cambridge University Press, Cambridge, England, 1992).
[8] P. Pieranski and E. Guyon, Phys. Rev. A **9**, 404 (1974).
[9] P. Manneville and E. Dubois Violette, J. Phys. **37**, 285 (1976).
[10] A. Polimeno and A. F. Martins, Liq. Cryst. **25**, 545 (1998).

[11] A. Polimeno, L. Orian, P. L. Nordio, and A. F. Martins, Mol. Cryst. Liq. Cryst. **336**, 17 (1999).
[12] A. Polimeno, L. Orian, A. F. Martins, and A. E. Gomes, Phys. Rev. E **62**, 2288 (2000).
[13] A. F. Martins, A. E. Gomes, A. Polimeno, and L. Orian, Phys. Rev. E **62**, 2301 (2000).
[14] C. J. Dunn, D. Ionescu, N. Kunimatsu, G. R. Luckhurst, L. Orian, and A. Polimeno, J. Phys. Chem. B **104**, 10989 (2000).
[15] A. F. Martins, A. E. Gomes, L. Orian, and A. Polimeno, Mol. Cryst. Liq. Cryst. **351**, 135 (2000).
[16] H. Siebert, D. A. Grabowski, and C. Schmidt, Rheol. Acta **36**, 618 (1997).
[17] L. Orian, A. G. Feio, A. Veron, A. Polimeno, and A. F. Martins, Mol. Cryst. Liq. Cryst. **394**, 63 (2003).
[18] E. Fischer and P. T. Callaghan, Phys. Rev. E **64**, 011501 (2001).
[19] P. T. Callaghan, Rep. Prog. Phys. **62**, 599 (1999).
[20] P. J. B. Edwards, M. Kakubayashi, R. Dykstra, S. M. Pascal, and M. A. K. Williams, Biophys. J. **98**, 1986 (2010).
[21] P. Callaghan, *Principles of Nuclear Magnetic Resonance Microscopy* (Oxford University Press, New York, 1994).
[22] Y.-F. Maa and C. C. Hsu, Biotechnol. Bioeng. **51**, 458 (2000).